

RESEARCH ARTICLE

Multi-Lineage Differentiation of Human Umbilical Cord Wharton's Jelly Mesenchymal Stromal Cells Mediates Changes in the Expression Profile of Stemness Markers

Hamad Ali^{1,2}, Majda K. Al-Yatama³, Mohamed Abu-Farha⁴, Kazem Behbehani¹, Ashraf Al Madhoun^{1*}

1 Department of Basic Science Research, Dasman Diabetes Institute, 1180 Dasman, Kuwait, **2** Department of Medical Laboratory Sciences (MLS), Faculty of Allied Health Sciences, Health Sciences Center, Kuwait University, Kuwait City, Kuwait, **3** Dar Al Baraa Medical Center, 3357 Hawally, Kuwait, **4** Biochemistry and Molecular Biology Unit, Dasman Diabetes Institute, 1180 Dasman, Kuwait

* ashraf.madhoun@dasmaninstitute.org



OPEN ACCESS

Citation: Ali H, Al-Yatama MK, Abu-Farha M, Behbehani K, Al Madhoun A (2015) Multi-Lineage Differentiation of Human Umbilical Cord Wharton's Jelly Mesenchymal Stromal Cells Mediates Changes in the Expression Profile of Stemness Markers. PLoS ONE 10(4): e0122465. doi:10.1371/journal.pone.0122465

Academic Editor: Zoran Ivanovic, French Blood Institute, FRANCE

Received: July 24, 2014

Accepted: February 11, 2015

Published: April 7, 2015

Copyright: © 2015 Ali et al. This is an open access article distributed under the terms of the [Creative Commons Attribution License](https://creativecommons.org/licenses/by/4.0/), which permits unrestricted use, distribution, and reproduction in any medium, provided the original author and source are credited.

Data Availability Statement: All relevant data are within the paper and its Supporting Information files.

Funding: RA-2013-009 and 2012-1302-03, www.kfas.org, Kuwait Foundation for the Advancement of Sciences, for AAM and HA, respectively. OMICSRU grant SRUL02/13 for HA. The funders had no role in study design, data collection and analysis, decision to publish, or preparation of the manuscript.

Competing Interests: The authors have declared that no competing interests exist.

Abstract

Wharton's Jelly- derived Mesenchymal stem cells (WJ-MSCs) have gained interest as an alternative source of stem cells for regenerative medicine because of their potential for self-renewal, differentiation and unique immunomodulatory properties. Although many studies have characterized various WJ-MSCs biologically, the expression profiles of the commonly used stemness markers have not yet been addressed. In this study, WJ-MSCs were isolated and characterized for stemness and surface markers expression. Flow cytometry, immunofluorescence and qRT-PCR analysis revealed predominant expression of CD29, CD44, CD73, CD90, CD105 and CD166 in WJ-MSCs, while the hematopoietic and endothelial markers were absent. Differential expression of CD 29, CD90, CD105 and CD166 following adipogenic, osteogenic and chondrogenic induction was observed. Furthermore, our results demonstrated a reduction in CD44 and CD73 expressions in response to the tri-lineage differentiation induction, suggesting that they can be used as reliable stemness markers, since their expression was associated with undifferentiated WJ-MSCs only.

Introduction

In recent years, the biological and clinical interest in Mesenchymal stem cells (MSCs) has increased noticeably due to their unique stemness characteristics. MSCs are non-hematopoietic cell population with multipotent precursor properties which has high degree of self-renewal and exhibit multi-lineage differentiation potential [1]. Although, MSCs reside primarily in the bone marrow, where they were first characterized [2]; studies have shown broad post-natal organ distribution of MSCs compartment including brain, liver, kidney, lung, adipose and connective tissues [3], as well as fetal tissues such as placenta, umbilical cord blood and matrix [4,

5] Unlike embryonic stem cells, the use of MSCs for clinical applications is ethically acceptable and no risk is associated with teratoma formation [6].

MSCs are described as immunologically privileged cells, modulate immune responses and exhibit anti-inflammatory properties (best reviewed in [7, 8]). MSCs lack the expression of the co-stimulatory surface antigens CD40, CD86 and CD80 that mediate T-cell activation [9–11] and suppress stimulated T-cells by activating TNF- α /NF- κ B signaling pathway [12]; and/or secreting soluble factors such as Eph/ephrin [13], prostaglandin E₂ [14] or indoleamine 2,3-dioxygenase [15]. MSCs drastically inhibit B-cell proliferation, differentiation and chemotactic behavior [16]. MSCs restrain the proliferation, maturation and activation of the innate immune system components, natural killer and dendritic cells. In the presence of MSCs, the secretory cytokine profile and molecules related to antigen presentation of these cells are inhibited [17, 18]. Thus, the recipient immunological tolerance to the administration of MSCs makes them ideal for clinical practice and good potential for cell therapy.

Currently, studies are focusing on adult bone marrow as a source for MSCs that suffers from a number of clinical limitations such as invasive collection procedures, the availability of suitable cell donors, poor mobility, limited long-term proliferation potential and age-limited frequency and differentiation capacity [19, 20]. Accordingly, there is a need to find other source of MSCs that possess similar characteristics of bone marrow MSCs but conquer these limitations.

Human umbilical cord blood (UB-MSCs) and Wharton's jelly (WJ-MSCs) stem cells are conventional model of choice for the development of potential novel cellular therapies (Fig 1A). Similar to adult MSCs, these cells acquire the stemness defined characteristics including multipotent differentiation potential, specific surface antigen expression and adherence to plastic [21]. Both UB- and WJ-MSCs are easy to collect from umbilical cord, which is considered as a medical waste, with painless noninvasive isolation procedure and no associated ethical constraints [22–24]. Although, a large donor pool is available, UB-MSCs are less attractive for clinical application due to their low frequency, poor proliferation rate and culture limitations [6].

WJ-MSCs are myofibroblastoid stromal cells isolated from the gelatinous layer within the umbilical cord tissue. The young WJ-MSCs are proliferative, immunosuppressive and remarkably stable under cultural conditions [25, 26]. Gene expression profiling studies revealed that WJ-MSCs share molecular signature similar to that of embryonic stem cells [27]. Relative to adult MSCs, a higher expression of the pluripotency markers like NANOG, Oct 3/4 and Sox2 were observed in cultured WJ-MSCs [28–30].

WJ-MSCs do not express a unique surface marker but rather express several markers that determine their identity as described by the guidelines recommendations of the International Society for Cellular Therapy (ISCT) for the characterization of MSCs [21]. WJ-MSCs are positive for surface antigens including the cell adhesion receptors, integrin β 1 (CD29 [31]) and the homing receptor (CD44, hyaluronan receptor [32]); the GPI-anchored protein, ecto-5'-nucleotidase (CD73 [33]); and thy-1 (CD90 [34]), signal transduction molecules and mediators of cell-cell and cell-matrix interactions; the intercellular adhesion molecule-1, ICAM-1 (CD54 [35]); TGF- β receptor binding glycoprotein, endoglin (CD105 [36]); the activated leukocyte cell adhesion molecule, ALCAM (CD166 [37]); the decay-accelerating factor (CD55 [35]), and the type II integral membrane protein (CD13 [35]). Further, WJ-MSCs are negative for the expression of the hematopoietic surface antigens CD14, CD45, CD34 and the endothelial markers CD106 and CD133 [1, 25, 38].

The aim of this study was to isolate and characterize WJ-MSCs from umbilical cords of end-term birth. A detailed description of the stem cell plasticity, their capacity to differentiation into adipogenic, osteogenic and chondrogenic lineages and the associated markers during

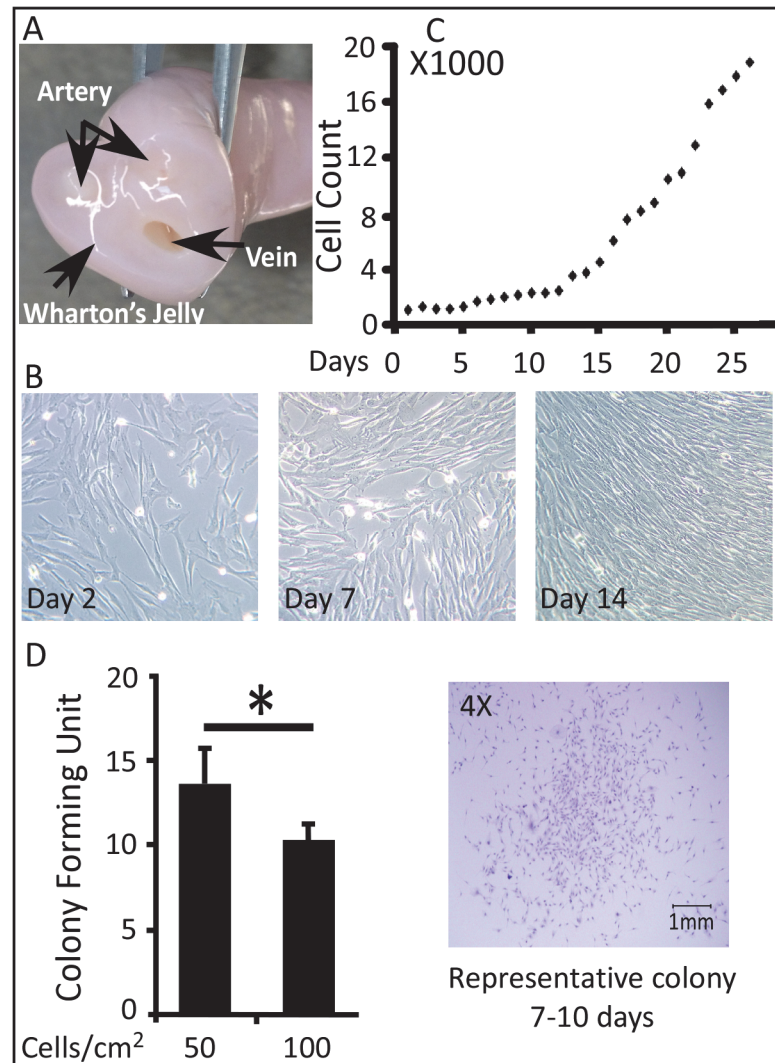


Fig 1. Source, Morphology and Growth Kinetics of WJ-MSCs. (A) The umbilical cord compartments. (B) Representative phase-contrast images of WJ-MSCs at Day 2, 7 and 14; 400X magnifications. (C) Growth rate, WJ-MSCs were seeded at a density of 1000 cells/cm², cellular proliferation was detected in a daily bases. (D) CFU-F, cells were plated at a density of 50 or 100 cells/cm² for 7–10 days. CFU-F was determined by (number of colonies formed/number of cells inoculated) x 100. *P < 0.05; the significance was evaluated by Student's *t*-test.

doi:10.1371/journal.pone.0122465.g001

the differentiation process was studied. For the first time, we explored WJ-MSCs stemness surface markers differential profile during the multi-lineage differentiation procedures.

Materials and Methods

Ethic Permission and Procurement of Human Samples

The study was pre-approved by the Ethical Review Committee at the Dasman Diabetes Institute (protocol No: 2013–009) in accordance with the World Medical Association Declaration of Helsinki- Ethical Principles for Medical Research Involving Human Subjects. Human umbilical cords were collected from a full-term natural delivery healthy infants after obtaining written informed consents from the mothers (age 20–30 years old) and family using the guidelines

recommended by the Ethical Review Committee. Umbilical cords (5–10 cm in length) were collected immediately after birth in sterile surgical tubes, transported to the laboratory, stored at -40°C and processed within 18 hrs.

Isolation and Culture of WJ-MSC from Human Umbilical Cords

WJ-MSC were isolated and cultured as described [39–41] with modifications. Umbilical cords were washed three times with phosphate buffer saline (PBS) containing penicillin (200 units/ml), streptomycin (200 $\mu\text{g}/\text{ml}$) and amphotericin B (5 $\mu\text{g}/\text{ml}$) to remove blood cells. Then, the umbilical cords were cut into 2–3 cm pieces, and each piece was transected longitudinally and the blood vessels were dissected. Wharton's jelly tissue was diced into small pieces and transferred into 15 ml tubes containing DMEM/Hams's F-12 (1:1 vol/vol) culture medium supplemented with 10% MSC-qualified FBS, collagenase type B (1 $\mu\text{g}/\text{ml}$), penicillin (100 units/ml), streptomycin (100 $\mu\text{g}/\text{ml}$), and amphotericin-B (2.5 $\mu\text{g}/\text{ml}$); cell culture media and supplements are purchased from Invitrogen. The tissue was digested at 37°C in a gentle orbital shaker until a tissue homogenate was obtained in approximately 4 hrs. The homogenate was centrifuged 500g for 20 minutes. The cell pellet was suspended in the described culture medium containing 10 ng/ml basic fibroblast growth factor (βFGF , R&D Systems), and with no collagenase. Cell proliferation was monitored during the first expansion period passage 0, (P0), for several days before the first passage (P1). Upon reaching 100% confluence, cells were detached using 0.05% trypsin / 0.02% EDTA in PBS for freeze down and further subcultures.

Growth Kinetic Characteristics

Growth kinetics experiments were performed as described [30, 40, 42]. The proliferation curve and the accumulative cell population doubling time were determined by culturing the cells to 80% confluence, harvesting, and counting at the indicated time points. Growth kinetics was evaluated by calculating accumulative population doubling time. Population doublings were calculated using the formula: $X = [\log_{10}(\text{N}_h) - \log_{10}(\text{N}_i)] / \log_{10}(2)$; where X is the population doubling; N_i is the inoculum number and N_h is the cell harvest number. The cumulative population doubling level was calculated by adding the population doubling for each passage to the population-doubling level of the previous passage. The population-doubling time was obtained by the formula: $\text{TD} = [t^* \log 2] / [\log(\text{N}_h) - \log(\text{N}_i)]$; where N_i is the inoculum cell number, N_h is the cell harvest number, and t is the time of the culture (in hours) [35].

Colony Forming Unit-Fibroblast (CFU-F)

CFU-F assays were performed as previously described [43] with some modifications. WJ-MSCs (P2- P5 from 3 different umbilical cord sources; 9-replicates each) were cultured at approximate densities of 50 and 100 cells/ cm^2 in 6 well plates. After 7–10 days, culture media was removed; cells were washed with 1X PBS and fixed with ice-cold methanol for 5 min. The plates were air dried, stained with 0.4% Trypan blue solution (Invitrogen) to be counted. The amount of colonies (1–8 mm in diameter) were established by scoring individual colonies derived from a single precursor using Stereo-microscope (Olympus, SDF plapo 1XPF). The plating efficiency was determined by the formula: (number of colonies formed/number of cells inoculated) X 100.

Flow Cytometry Analysis

A small fraction of Day 0, undifferentiated WJ-MSC, cells (passage 2–4, 10^5 cells) from at least 3 different preparations were analyzed using Flow cytometry (BD LSRII) for the expression of

Table 1. Primary Antibodies used for Flow Cytometry characterization of undifferentiated cells.

Antibody	Conjugate	Manufacturer	Catalogue number
CD29	AL700	Biolegend	303019
CD34	PE-Cy7	Biolegend	343515
CD44	Pacific Blue	Affymetrix eBioscience	48-0441
CD45	APC-Cy7	Biolegend	103115
CD73	Pacific Blue	Biolegend	344011
CD90	Fitc	Biolegend	328107
DC105	APC	Biolegend	323207
CD106	PE-Cy5	Biolegend	305808
CD133	APC	Miltenyl Biotec	130-098-829
CD166	Fitc	AbD Serotec	MCA1926F

doi:10.1371/journal.pone.0122465.t001

MSC surface markers using specific antibodies (Table 1) as described previously [44]. After addition of antibodies according to recommended concentrations, tubes were incubated in the dark at room temperature for 20 minutes; flow cytometry analysis was performed and then data analysis was done using BD FACSDiva software.

Western Blot and Immunofluorescence Assay

Western Blot assay was performed as described previously [45, 46]. Immunofluorescence assays were performed on undifferentiated- and adipogenic-differentiated WJ-MSC. WJ-MSCs differentiated into adipocytes were first Oil red-O stained as described below and then subjected to immunofluorescence assay. Cells were fixed with 4% paraformaldehyde for 15 min, washed extensively with PBS and then incubated overnight with the antibodies. Anti human-CD29 (R&D Systems) were conjugated with Alexa Fluor 594; were as anti human-CD44 (Novus-bio),-CD90 (R&D Systems) and-CD166 ((R&D Systems) were conjugated with Alexa Fluor 488 using APEX Antibody Labeling Kits (Invitrogen). Pre-conjugated anti-human CD105-PE (clone SN6), anti-human CD73-PE (clone AD2) were purchased from eBioscience. Fluorescent and phase contrast images were captured using Confocal Laser-Scanning microscope (Zeiss, LSM 710) as previously described [47].

RNA Extraction, cDNA Synthesis and qRT-PCR Reactions

Total RNA was extracted from cells using the total RNA purification kit (Norgen Biotek, Canada) following the manufacturer's protocol. First strand cDNA was synthesized from 50–100 ng RNA by reverse transcription using QuantiTect Reverse Transcription Kit (Qiagen Inc., USA). qRT-PCR reactions were performed as described [46, 48]. Primer pairs (Table 2) were selected from PrimerBank [49] and tested for equivalent efficiency. qRT-PCR was performed on the ABI7900 system (Applied Biosystems, USA) using SDS software. Relative gene expression was calculated using comparative Ct method as previously described [45, 50]. Results were normalized to GAPDH, and averages \pm SEM are shown expressed relative to Control or Day 0 undifferentiated cells, as indicated.

Proteomic Analysis

Proteomics were analyzed using LTQ-Orbitrap velos as described previously [51]. Briefly, peptides were suspended in 5% formic acid and then loaded on a C18-A1 easy column for desalting (Proxeon Biosystems, Denmark). Desalted peptides were then directed to a C18-A2 analytical easy column and eluted at a gradient of 5 to 35% acetonitrile with 0.1% formic acid

Table 2. Oligonucleotide sequences of primers utilized for real-time qRT-PCR.

Genes	Forward Primer (5'-3')	Reverse Primer (5'-3')
CD29	GTAACCAACCGTAGCAAAGGA	TCCCCTGATCTTAATCGCAAAAC
CD34	AATCAGCACAGTGTTCCACCAC	TGCCCTGAGTCAATTTCACTTC
CD44	CTGCCGCTTTGCAGGTGTA	CATTGTGGCAAGGTGCTATT
CD45	ATTACCTGGAATCCCCCTCAAA	TTGTGAAATGACACATTGCAGC
CD73	GCCTGGGAGCTTACGATTTTG	TAGTGCCCTGGTACTGGTTCG
CD90	ATCGCTCTCCTGCTAACAGTC	CTCGTACTGGATGGGTGAACT
CD105	TGCACTTGGCCTACAATTCCA	AGCTGCCCACTCAAGGATCT
CD106	GGGAAGATGGTCGTGATCCTT	TCTGGGGTGGTCTCGATTTTA
CD133	GGCCCACTACAACACTACCAA	ATTCCGCCTCTAGCACTGAA
CD166	ACTTGACGTACCTCAGAATCTCA	CATCGTCGACTGCACACTTT
GAPDH	GGAGCGAGATCCCTCCAAAAT	GGCTGTTGTCACTTCTCATGG
PPAR γ 2	ACCAAAGTGCAATCAAAGTGGA	ATGAGGGAGTTGGAAGGCTCT
Adiponectin	AACATGCCCATTCGCTTTACC	TAGGCAAAGTAGTACAGCCCA
Osteoprotegerin (OPG)	GTGTGCGAATGCAAGGAAGG	CCACTCCAAATCCAGGAGGG
Osteopontin	CTCCATTGACTCGAACGACTC	CAGGTCTGCGAAACTTCTTAGAT
Chondroadherin (CHAD)	GGACCACAACAAGTCACTGA	GTGGAATTTGGCGAGGTTCTC

doi:10.1371/journal.pone.0122465.t002

for 120 min (Proxeon Biosystems, Denmark). The full MS spectra scan was performed at a resolution of 60,000. MS/MS spectra were acquired in a data-dependant acquisition mode selecting top 20 spectra. Raw data files were analyzed using Maxquant 1.3.0.5 software (Thermo Scientific; Germany) using Sequest and Mascot search engine against the Homo sapiens International Protein Index (IPI) protein sequence database version 3.68 (European Bioinformatics Institute, United Kingdom).

WJ-MSC *in vitro* cellular differentiation

The *in vitro* lineages differentiation was performed on WJ-MSC (P2-P5) isolated from three different pregnancies and each differentiation experiment was done in triplicate, as described by Wang *et al.*, 2004, with modifications [52]. For RNA extractions and time point differentiation profile, cells were harvested on weekly bases till the end of each experiment.

Adipogenic differentiation. A 24 well plate was cultured with 2×10^4 cells/well. At 50–60% cell confluency, cells were treated with Adipogenic medium contained DMEM-low glucose supplemented with 10% FBS, penicillin (100 units/ml), streptomycin (100 μ g/ml), 1 μ M dexamethasone, 500 μ M isobutylmethylxanthine (IBMX), 5 μ g/ml insulin, 200 μ g/ml ascorbate-2-phosphate. The Culture medium was replaced every 3 days for 4-weeks period. At the end of the experiment weeks 3; cells were fixed in 4% paraformaldehyde for 15 min at room temperature, washed with sterile water and then with 60% isopropanol, finally, stained with 0.5% Oil red-O (Sigma) in isopropanol (wt/vol) for 30 min. Excess stain was removed and the cells were washed 3 times with sterile water. Control cells were grown in culture medium without inductive supplements.

Osteogenic Differentiation. A 24 well plate was cultured with 2×10^4 cells/well. At 80% cell confluency, cells were treated with osteogenic medium contained DMEM-low glucose supplemented with 10% FBS, penicillin (100 units/ml), streptomycin (100 μ g/ml), 100 nM dexamethasone, 10 mM β -glycerophosphate and 50 μ g/ml ascorbate-2-phosphate. The Culture medium was replaced every 3 days for 3-week period. Cells were fixed and osteogenesis was

detected using Alkaline phosphatase detection Kit (Millipore) following the manufacturer protocol. Control cells were grown in culture medium without inductive supplements.

Chondrogenic Differentiation. The protocol, described by Karahuseyinoglu *et al.*[53], was followed with some modification. 4×10^5 cells were centrifuged 1000 rpm for 10 minutes in 15 mL tubes. Chondrogenic medium was gently added without disturbing the cells pellet. Cells were allowed to form aggregates by incubating the tubes at 37°C in 5% CO₂ in a humidified environment. Chondrogenic medium contains DMEM-high glucose supplemented with 20 ng/ml TGF-β₃, 100 nM dexamethasone, 50 ng/ml Ascorbate-2-phosphate, 1 mM sodium pyruvate, 1X ITS (6.25 μg/ml Insulin, 6.25 μg/ml Transferrin, 6.25 ng/ml Selenous acid), 50 μg/ml proline. The cell aggregates were allowed to grow for 3 weeks. Cell spheres were fixed with 4% paraformaldehyde for 24 hrs at room temperature and then were stained with 1% Alcian Blue (Sigma Aldrich, Germany).

Statistical Analyses

In this study, umbilical cords were used from three different pregnancies. WJ-MSCs isolated from each umbilical cord were subjected to multi-lineage differentiation in three independent experiments. Statistical significance was estimated with a one-tailed Student's t-test assuming equal variance and error is s.e.m. (*P < 0.05) [48].

Results

Cell isolation, proliferation and Characterization of WJ-MSCs

Umbilical cords were stripped of the cord blood vessels and Wharton's jelly (WJ) matrixes were scabbed off into small pieces. WJ-MSCs were isolated using proteolytic enzyme digestion protocol and the cells were cultured in DMEM supplemented with 10% MSC-qualified FCS and 4 ng/mL bFGF. The freshly isolated WJ-MSCs grow as a flat monolayer and exhibit an elongated spindle-shape fibroblast-like morphology when cultured on polystyrene tissue culture plates (Fig 1B).

WJ-MSCs, seeded at a density of 1000 cells/cm², did not show changes in growth rates at the first 5 days in culture. The following days 6–12, the cells demonstrated significant low proliferation rates, with an average accumulative population doubling rate (APDR) of 1.3 ± 0.88 and the average population doubling time (PDT) was 33.1 ± 5.7 hrs. Notably, a robust proliferation rates were recorded at culture days 13–26; the observed average APDR and PDT were 6.2 ± 1.7 and 8.1 ± 2.6 hrs, respectively (Fig 1C).

To assess the capacity and frequency of self renewal WJ-MSCs; cells (P2-P5) were seeded in two density groups (50, and 100 cells/cm²) and the new forming fibroblast colonies derived from single cells were assessed after 7 to 10 days. As shown in Fig 1D, lowering the cell density improved CFU-F. 50 cells/cm² produced 13.4 ± 2.5 colonies which is significantly higher than the seeding density at 100 cells/cm² that generated 9.8 ± 0.8 CFU-F.

Further, we performed proteomic analysis on the isolated WJ-MSCs. Data analysis has shown the expression of several stemness proteins including Prohibitin, Gelsolin, EF-hand calcium-binding protein RLP49, and Solute carrier family 2 (S1 Dataset).

The expression of the CD- surface markers

Flow cytometry immune profiling, cell passage 3–5, revealed positive expression (>95%) for the putative mesenchymal stem markers CD29, CD44, CD73, CD90, CD105. The endothelial surface markers, CD106 and CD133, and the hematopoietic stem marker CD34 showed negative antigenic reactivity. While and the monocyte-macrophage CD45 marker showed minor

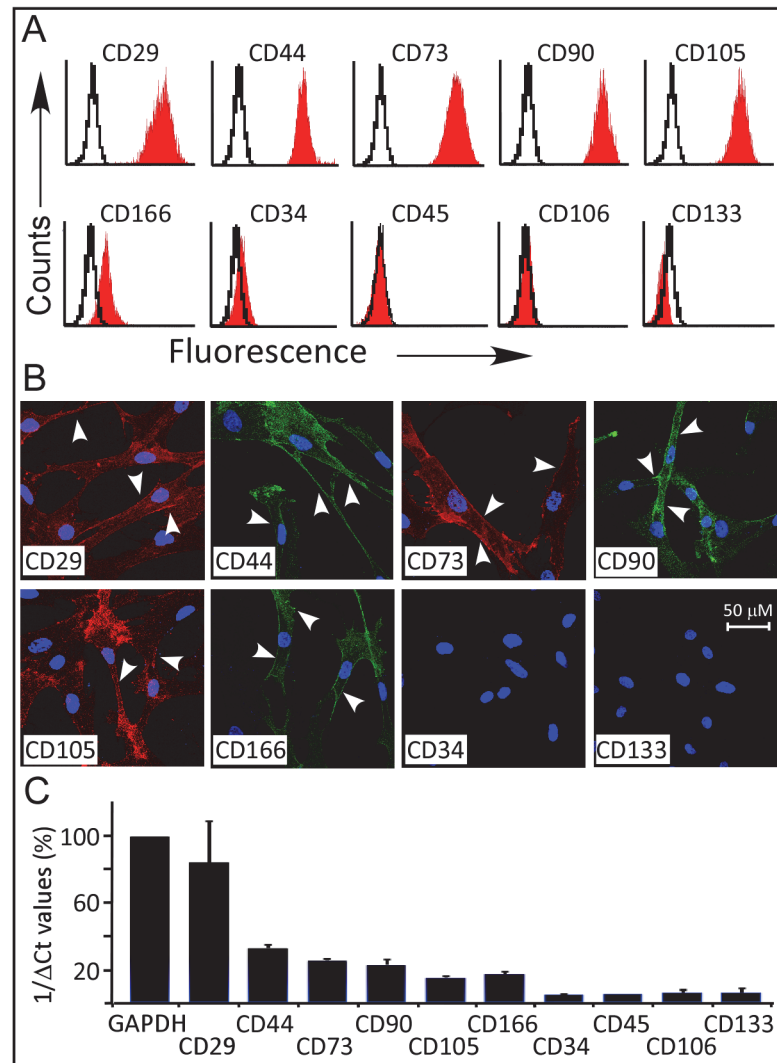


Fig 2. Flow cytometry, Immunofluorescence and qRT-PCR of WJ-MSCs. (A). Representative flow cytometry of WJ-MSCs (n = 3). Cells express CD29, CD44, CD73, CD90, CD105, and are negative for the hematopoietic (CD34 and CD45) and endothelial (CD106 and CD133) markers. Black open histogram indicates controls signal; red shaded histogram represents positive reactivity with the indicated antibody. (B) Confocal laser images of Immunofluorescence using APEX-labeling system for conjugating primary antibodies; CD29-Alexa Fluor 594, CD34-, CD44-, CD90- and CD133- Alexa Fluor 488. CD73-PE and CD105-PE were manufacturer labeled. 600X magnifications (C) qRT-PCR of the prospective markers for RNA isolated from undifferentiated WJ-MSCs cells, values were expressed as a percentage relative to 1/dCt of GAPDH gene.

doi:10.1371/journal.pone.0122465.g002

reactivity (<5%), suggesting a minor contamination with hematocytes (Fig 2A). The expression of the surface markers was also observed by immunofluorescence analysis using anti-human CDs antibodies as described in Fig 2B (and S1 Fig). Confocal laser microscopy images show the cell membrane localization of the tested surface markers (arrowheads).

In accordance with the flow cytometry data, real time quantitative reverse transcriptase-polymerase chain reaction (qRT-PCR) analysis demonstrated statistically significant high gene expression levels of the integrin marker CD29 (82% relative to GAPDH). The expression levels of the matrix markers (CD44 and CD105), CD73 and CD90 were 15%- 38% relative to that of

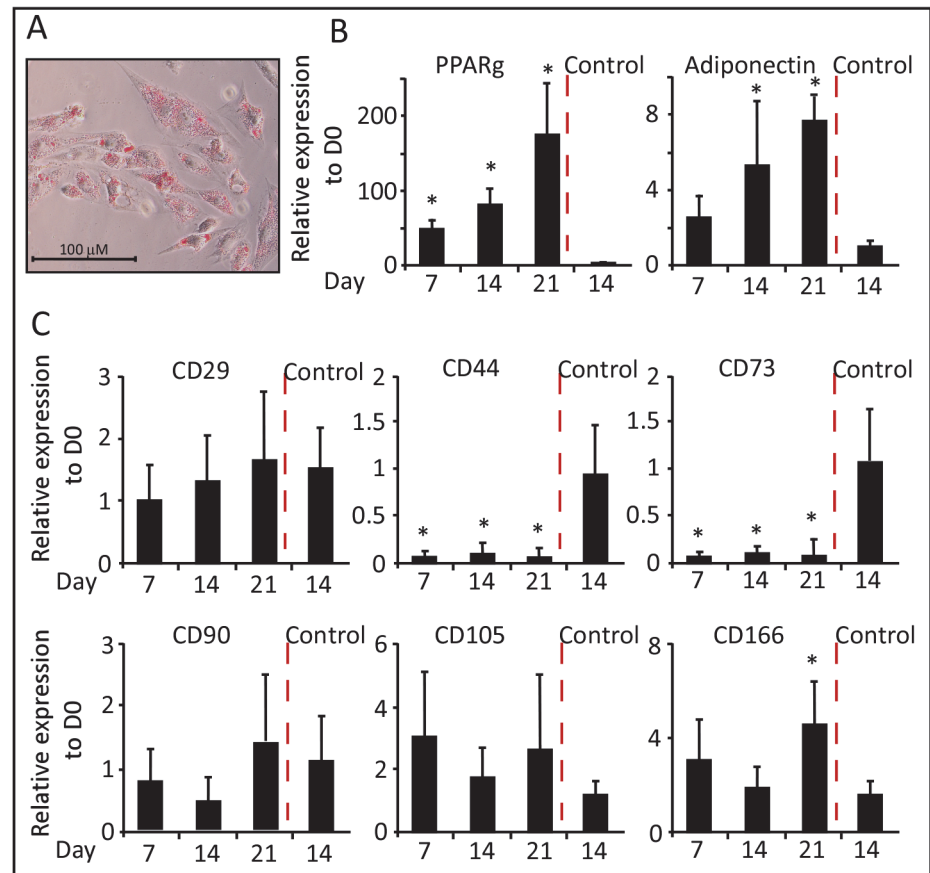


Fig 3. Adipogenic differentiation of WJ-MSCs. (A) Representative staining of adipocytes with Oil Red-O stain (200X). (B) and (C) qRT-PCR was performed after the induction of adipogenic differentiation of WJ-MSCs. Results for all panels were expressed as fold-change relative to Day 0—undifferentiated WJ-MSCs (n = 3, *p < 0.05).

doi:10.1371/journal.pone.0122465.g003

GAPDH. Low RNA expression (<4% relative to GAPDH) was detected for the hematopoietic and endothelial markers (Fig 2C).

Multi-lineage differentiation capabilities of WJ-MSCs

According to ISCT guidelines, WJ-MSCs should exhibit the multi-lineage differentiation potential (adipogenic, osteogenic and chondrogenic), in order to be legitimate as functional MSCs. We studied the tri-lineage differentiation potential of WJ-MSCs and characterized the cellular markers in time dependent fashion. The differentiation potential was limited to cell passages 3–5.

Adipogenic differentiation. In order to investigate the potential of WJ-MSCs differentiation into adipocytes; cells were treated with IBMX, dexamethasone and insulin for a period of three weeks. Cells were harvested at days 7, 14 and 21 for RNA extraction and qRT-PCR analysis using specific primers for the studied markers (Table 2). On Day 21 of differentiation, adipocytes were detected by Oil Red-O positive staining of lipid droplets (Fig 3A). At molecular level, qRT-PCR analysis demonstrated a significant time course dependent increase in the expression of adipogenic markers peroxisome proliferator-activated receptor gamma (PPARγ) and adiponectin (Fig 3B), as compared to control-treated cells, which did not differentiate efficiently into adipocytes.

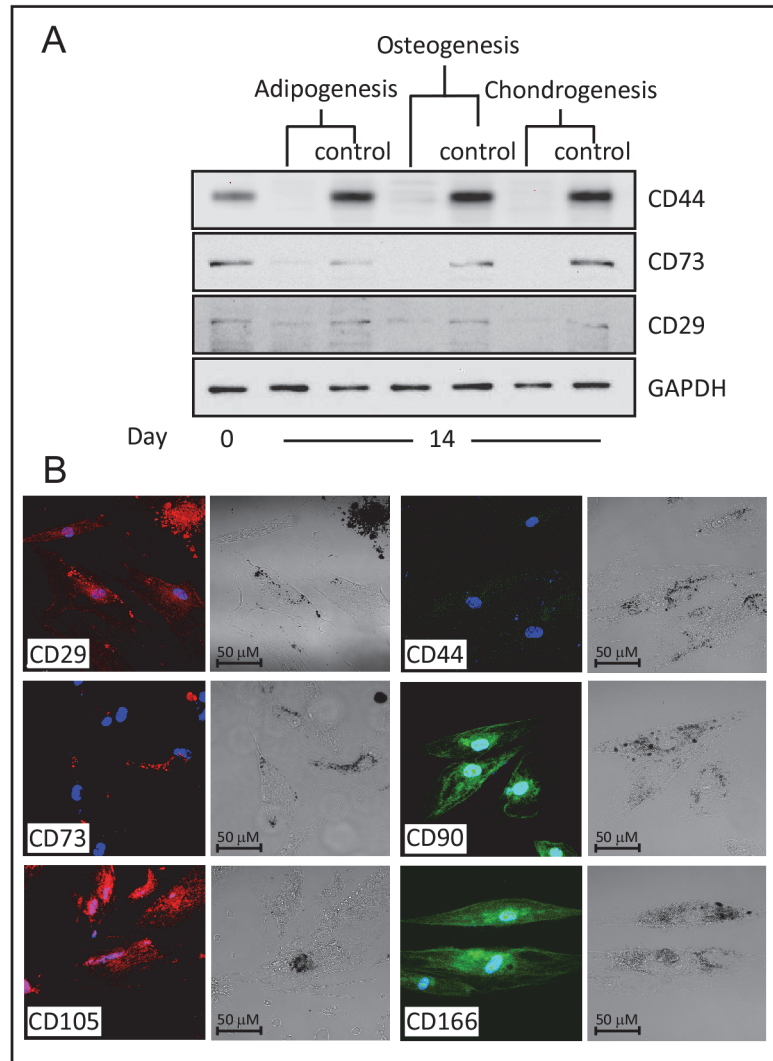


Fig 4. Protein expression of CD-markers during multi-lineage differentiation. (A) Western Blot analysis of undifferentiated (D0) and multi-lineage differentiated WJ-MSCs (D14). (B) Adipogenic differentiation of WJ-MSCs, immunofluorescence images using Confocal Laser microscopy (400X magnification). Primary antibodies were conjugated as described in Material and Methods. CD29-Alexa Fluor 594, CD44-, CD90- and CD166-Alexa Fluor 488, CD-73- and CD105-PE. Oil Red-O staining was observed as black dots using monochrome digital camera (phase contrast images) or red dots using 633-nm Laser beam.

doi:10.1371/journal.pone.0122465.g004

To determine the authenticity of the stemness markers that characterize MSC, we studied the gene expression of these markers during the differentiation process. Interestingly, the transcript level of CD29 was equivalent to that of undifferentiated cells and day 14-control cells (Fig 3C). The expression of CD105 and CD166 showed a non significant 2–4 fold increase as compared to undifferentiated cells. The expression of CD90 was moderately reduced in the first two weeks, but then elevated at equivalent levels to that of the controls. Both CD44 and CD73 gene expression was dramatically reduced though out the course of differentiation (Fig 3C). In accordance with the gene expression analysis, a similar expression pattern of proteins from total cellular extracts of WJ-MSC- undifferentiated (D0) versus differentiated into adipocytes was detected (Fig 4A). Western Blot analysis, using specific antibodies against the CD

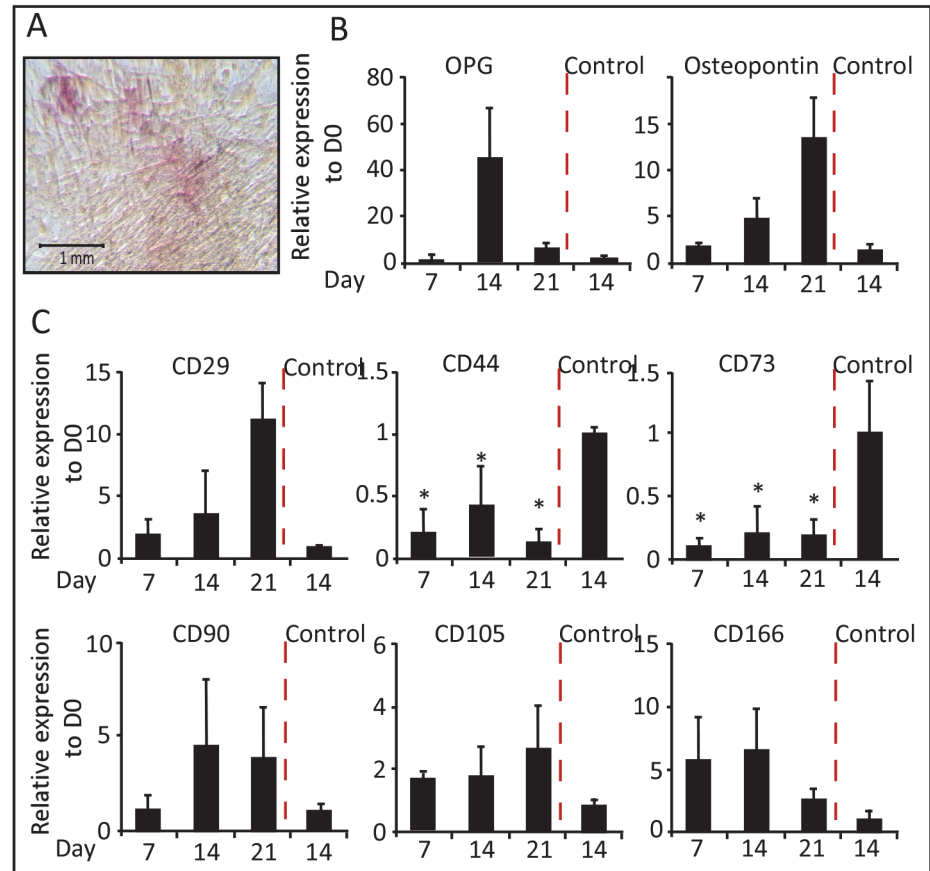


Fig 5. Osteogenic differentiation of WJ-MSCs. (A) Representative staining of osteoblast with alkaline phosphatase reactivity staining (100X). (B) and (C) qRT-PCR was performed after the induction of osteogenic differentiation of WJ-MSCs. Results for all panels were expressed as fold-change relative to Day 0—undifferentiated WJ-MSCs (n = 3, *p < 0.05).

doi:10.1371/journal.pone.0122465.g005

markers, revealed a dramatic reduction in protein levels of CD44 and CD73, whereas the CD29 protein was sustained during adipogenesis.

The protein expression of the CD-markers was also visualized using immunofluorescence images post adipogenic differentiation of WJ-MSCs (Fig 4B), which was marked by Oil Red-O staining (observed as black dots in phase contrast images using monochrome camera, and as red spots under 633-nm Laser ray, e.g. CD73 images, Fig 4B). Unlike CD29, CD90, CD105 and CD166; the cell membrane expressions of CD44 and CD73 were not detected (Fig 4B), supporting the data obtained from molecular studies.

Osteogenic Differentiation. The osteogenic differentiation of WJ-MSCs was determined by culturing them in media containing dexamethasone, β -glycerophosphate and ascorbate as described in Material and Methods section. RNA was extracted at days 7, 14 and 21 during the differentiation time course. On day 21 of differentiation, cells showed remarkable changes in cellular morphology and were stain positive for alkaline phosphatase activity (Fig 5A) and von Kossa staining of calcified bone matrix (data not shown). qRT-PCR analysis showed that the expression of osteoprotegerin (OPG) and osteopontin transcripts increased during the differentiation, almost 50-fold by day 14 and 15-fold by day 21, respectively (Fig 5B).

Similar to our observation during adipogenesis; CD29 and CD90 gene expressions were gradually increased during the differentiation time course and peaking at day 21. Whereas,

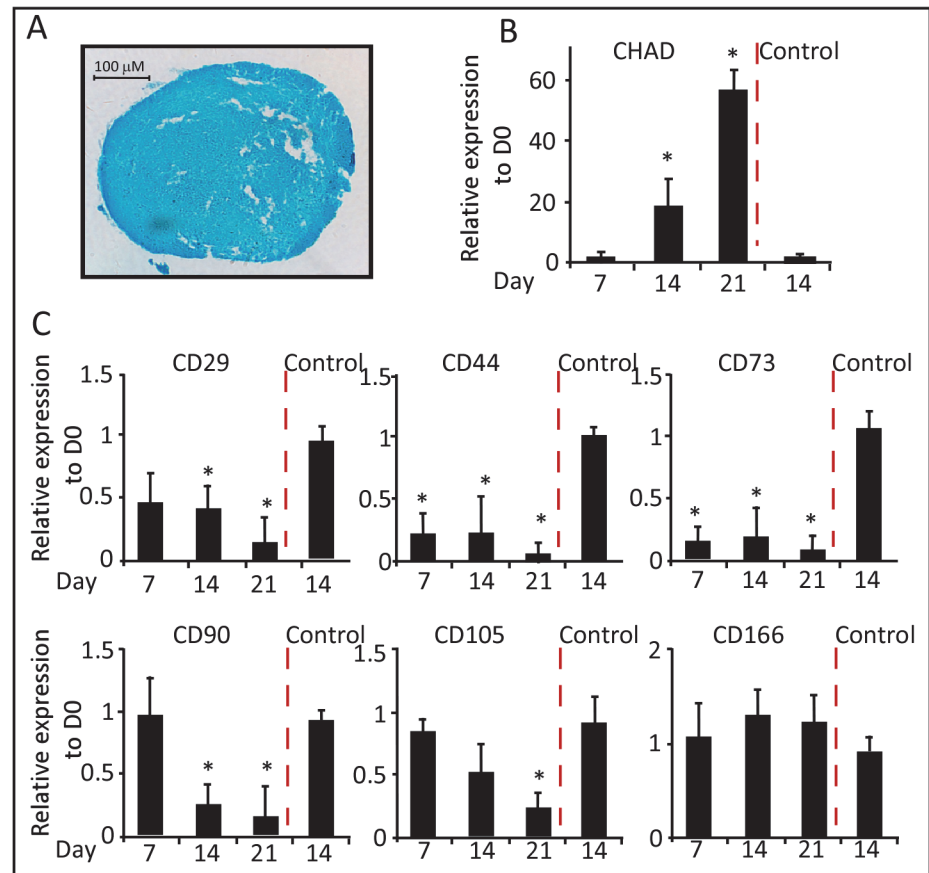


Fig 6. Chondrogenic differentiation of WJ-MSCs. (A) Representative staining of chondrocytes with Alcian Blue staining (200X). (B) and (C) qRT-PCR was performed after the induction of chondrogenic differentiation of WJ-MSCs. Results for all panels were expressed as fold-change relative to Day 0—undifferentiated WJ-MSCs (n = 3, *p < 0.05).

doi:10.1371/journal.pone.0122465.g006

CD105 and CD166 showed constant gene expression with 2 to 5-fold enhancement compare with control cells. On the other hand, CD44 and CD73 transcripts levels were 50 to 90% lower than the transcript level of control cell lines (Fig 5C). Subsequent Western blot analysis showed absences of CD44 and CD73 expressions, but not CD29, during osteogenesis relative to controls (Fig 4A).

Chondrogenic Differentiation. Chondrogenic differentiation was induced by aggregating WJ-MSCs in a serum free media containing TGF-β3, dexamethasone and ITS; for a period of three weeks. Following, two days culture in canonical tubes, the cell pellets lost attachment and formed spherical aggregates which increased in size indicating the production of extracellular matrix. Cell aggregates were harvested at days 7, 14 and 21 for gene expression. On day 21 of differentiation, cell aggregates were stained with Alcian blue a marker for glycosaminoglycans in cartilages (Fig 6A). qRT-PCR analysis of the chondrogenic marker chondroadherin (CHAD); showed a 20- and 60-fold increase in RNA expression at days- 14 and 21 of differentiation, respectively (Fig 6B).

Different gene expression patterns were detected for the stemness markers during chondrogenesis. Relative to the control cells, CD29 and CD90 transcripts were reduced after 7- and 14-days of chondrogenic induction, respectively (Fig 6C). The RNA levels of CD166 were maintained; while those of CD105 were gradually reduced during the differentiation time course.

Similar to the other lineages, the expression levels of CD44 and CD73 RNAs were noticeably reduced as compared to undifferentiated cells (Fig 6C). These data were further supported using Western blot analysis, the protein expressions of CD29, CD44 and CD73 were noticeably reduced in response to chondrogenic differentiation (Fig 4B).

Discussion

MSCs have proven to represent a major hope for cell-based therapy and tissue engineering applications, as these cells possess the capacity for self-renewal and multi-lineage differentiation potentials [54, 55]. In addition, MSCs can be used for clinical applications due to their immunomodulatory properties [56]. MSCs are isolated from several postnatal and extra-embryonic tissues, which are discarded as medical wastes and thus do not provoke technical or ethical concerns [52, 57]. Currently, similar to other MSCs, it is well established that WJ-MSCs express a wide range of surface antigen markers including CD29, CD44, CD73, CD90, CD105 and CD166; and lack the expression of the hematopoietic or endothelial markers [58]. However, in WJ-MSCs, there are no studies tracing the expression profile of these markers during the differentiation processes. In this study, we report the isolation and characterization WJ-MSCs that inhabit the gelatinous portion of the umbilical cord. Further, we have elucidated the molecular profile of the commonly used stemness surface markers associated with WJ-MSCs differentiation.

WJ-MSCs displayed robust proliferation abilities. The growth curve of isolated cells revealed a characteristic pattern. In the first 12 days, cells showed a slow proliferation profile and then entered the logarithmic growth phase which continued for 14 days. It is reputable that self-renewal and high proliferation capacity are critical for MSCs to maintain stemness characteristics during *in vitro* culturing [59]. Using the isolated WJ-MSCs, a systematic evaluation of the effect of plating density on CFU-F was performed. The cell seeding density was negatively correlated with the observed CFU-F frequency, suggesting a possible paracrine signaling or metabolic products that may reduce clonogenic frequency or down-regulate WJ-MSCs proliferation [60, 61].

In addition, we utilized the proteomic approach to further characterize the stemness authenticity of the isolated WJ-MSCs. Mass spectroscopy analysis revealed that these cells express proteins that have been previously identified to be stem cell related [25, 62–64]. With particular interest, two prohibitin proteins were identified PhB1 and PhB2; the former is reported to be crucial for the regulation of embryonic stem cells homeostasis and differentiation [65]. On the other hand, Gelsolin has been recognized as an important checkpoint in the differentiation of MSCs under the regulation of TGF- β [66].

In accordance with previous reports, we found that the undifferentiated WJ-MSCs co-express the stemness markers CD29, CD44, CD73, CD90, CD105 and CD166. qRT-PCR analysis revealed that CD29 is much more strongly expressed as compared to the other markers. Interestingly, the expression profile of these markers showed a distinctive pattern during the multi-lineage differentiations.

The transcripts of the transmembrane proteins integrin β 1 subunit (CD29) and the Thy-1 (CD90) were found to be up-regulated and down-regulated upon the onset of osteogenic and chondrogenic lineages, respectively; with more prominent expression profile after three weeks of differentiations. CD29 and its modulator ICAP-1 are required for osteoblast proliferation and differentiation explaining the observed increase in its expression during osteogenesis [67]. Our results confirm previous reports observing down regulation of CD90 during differentiation in human bone marrow MSCs (BM-MSCs) [41, 68, 69], and synovium derived MSCs [70]. We observed a steady upregulation of CD29 expression during adipogenic differentiation, but

CD90 transcripts were reduced, supporting previous reports indicating that CD90 is negatively correlated with adipogenesis [71]. CD105, also called endoglin, is a type I membrane glycoprotein receptor that is a part of the transforming growth factor β (TGF β) receptor complex. The expression of CD105 was moderately upregulated during adipogenic and osteogenic; but not chondrogenic differentiation. Treatment with TGF β induces chondrogenesis and is associated with CD105 low protein expression in human bone marrow MSCs (BM-MSCs) cultured on micromass and alginate systems [68, 69, 72].

CD166 with adhesive properties belongs to the type I transmembrane glycoprotein as a member of the immunoglobulin super-family of protein. Similar to the previously reported proteomic studies on human BM-MSCs [35], we found that the expression of CD166 is upregulated during adipogenic and osteogenic differentiations. No changes in the expression profile of CD166 were detected in cells undergoing chondrogenesis. These results contradict a previous data showing that CD166 protein is down-regulated during chondrogenic differentiation in BM-MSCs. The discrepancy can be explained by the differences in BM- versus WJ-MSCs, or explained by possible post translational regulations that causes lower rates of protein translation compare to RNA transcription.

Interestingly, the expression levels of CD44 and CD73 were dramatically reduced during the multi-lineage differentiation process. Protein studies have shown that the hyaluronan receptor, CD44, is down regulated during chondrogenesis and osteogenesis in human BM-MSCs [35, 69]. CD73, on the other hand, was reported to be slightly increased in human BM-MSCs undergoing adipogenic and osteogenic differentiation [35].

Our focus on the commonly used MSCs markers and tracking their expression profile during multi-lineage differentiation may provide key insights on WJ-MSCs signature. Currently, there is no single molecule or protein that can be used for WJ-MSCs identification and isolation. Interestingly, the commonly used positive markers are selected to include surface antigens that are absent from most hematopoietic cells, which might be beneficial to isolate BM-MSCs, but not MSCs from other tissues. The existence of CD29, CD90, CD105 and CD166 transcripts in terminally differentiated cells, suggests that these markers may not be ideal markers to identify and isolate WJ-MSCs, since the later cells are impeded in a tissue layer rich in adipogenic-, smooth muscle- and vascular tissues. On the contrary, the low expression levels of CD44 and CD73 during multi-lineage differentiation imply that these two markers have low cellular abundance; at least in part, at the tri-lineages studied. Thus, CD44 and CD73 are reliable stemness markers for WJ-MSCs, since their expression is associated with undifferentiated WJ-MSCs only.

Supporting Information

S1 Dataset. Proteomic analysis of undifferentiated WJ-MSCs. Total proteins were extracted and digested. The generated peptides were subjected for MS/MS analysis. The generated spectra were acquired in a data-dependant acquisition mode selecting top 20 spectra. Raw data files were analyzed using Maxquant 1.3.0.5 software using Sequest and Mascot search engine against the Homo sapiens International Protein Index (IPI) protein sequence database version 3.68 (European Bioinformatics Institute, United Kingdom). Stem cell specific proteins which were previously reported are list and referenced. (XLSX)

S1 Fig. Immunofluorescence analysis for undifferentiated WJ-MSCs. Cells were incubated with antibodies directed against the individual surface markers. Confocal laser images of Immunofluorescence using APEX-labeling system for conjugating primary antibodies; CD29-Alexa Fluor 594, CD34-, CD44-, CD90- and CD133- Alexa Fluor 488. CD73-PE and

CD105-PE were manufacturer labeled. Phase contrast images 600X magnifications. Nuclei are stained with Hoechst. The CD-markers proteins are located at the cell member as observed by the Immunofluorescence.

(TIF)

Acknowledgments

We thank Ms. Valerie Lopez Atizado, Tissue Banking unit-Dasman Diabetes Institute, for processing the samples presented at [Fig 6A](#). We thank Dr. Jehad Abubakr for critical comments and discussions on the manuscript.

Author Contributions

Conceived and designed the experiments: HA AAM. Performed the experiments: HA MAF AAM. Analyzed the data: HA KB AAM. Contributed reagents/materials/analysis tools: MKA KB AAM. Wrote the paper: AAM. Obtained permission for use of WJ-MSCs: KB AAM.

References

1. Pittenger MF, Mackay AM, Beck SC, Jaiswal RK, Douglas R, Mosca JD, et al. Multilineage potential of adult human mesenchymal stem cells. *Science*. 1999; 284(5411):143–7. PMID: [10102814](#)
2. Friedenstein AJ, Chailakhjan RK, Lalykina KS. The development of fibroblast colonies in monolayer cultures of guinea-pig bone marrow and spleen cells. *Cell Tissue Kinet*. 1970; 3(4):393–403. PMID: [5523063](#)
3. Meirelles LDS, Chagastelles PC, Nardi NB. Mesenchymal stem cells reside in virtually all post-natal organs and tissues. *J Cell Sci*. 2006; 119(11):2204–13. PMID: [16684817](#)
4. Jiang R, Han Z, Zhuo G, Qu X, Li X, Wang X, et al. Transplantation of placenta-derived mesenchymal stem cells in type 2 diabetes: a pilot study. *Front Med*. 2011; 5(1):94–100. doi: [10.1007/s11684-011-0116-z](#) PMID: [21681681](#)
5. Martins AA, Paiva A, Morgado JM, Gomes A, Pais ML. Quantification and immunophenotypic characterization of bone marrow and umbilical cord blood mesenchymal stem cells by multicolor flow cytometry. *Transplant Proc*. 2009; 41(3):943–6. doi: [10.1016/j.transproceed.2009.01.059](#) PMID: [19376394](#)
6. Zeddou M, Briquet A, Relic B, Josse C, Malaise MG, Gothot A, et al. The umbilical cord matrix is a better source of mesenchymal stem cells (MSC) than the umbilical cord blood. *Cell Biol Int*. 2010; 34(7):693–701. doi: [10.1042/CBI20090414](#) PMID: [20187873](#)
7. Bassi EJ, Aita CA, Camara NO. Immune regulatory properties of multipotent mesenchymal stromal cells: Where do we stand? *World J Stem Cells*. 2011; 3(1):1–8. doi: [10.4252/wjsc.v3.i1.1](#) PMID: [21607131](#)
8. Law S, Chaudhuri S. Mesenchymal stem cell and regenerative medicine: regeneration versus immunomodulatory challenges. *Am J Stem Cells*. 2013; 2(1):22–38. PMID: [23671814](#)
9. Maccario R, Podesta M, Moretta A, Cometa A, Comoli P, Montagna D, et al. Interaction of human mesenchymal stem cells with cells involved in alloantigen-specific immune response favors the differentiation of CD4(+), T-cell subsets expressing a regulatory/suppressive phenotype. *Haematol-Hematol J*. 2005; 90(4):516–25.
10. Devine SM, Cobbs C, Jennings M, Bartholomew A, Hoffman R. Mesenchymal stem cells distribute to a wide range of tissues following systemic infusion into nonhuman primates. *Blood*. 2003; 101(8):2999–3001. PMID: [12480709](#)
11. Tse WT, Pendleton JD, Beyer WM, Egalka MC, Guinan EC. Suppression of allogeneic T-cell proliferation by human marrow stromal cells: Implications in transplantation. *Transplantation*. 2003; 75(3):389–97. PMID: [12589164](#)
12. Dorronsoro A, Ferrin I, Salcedo JM, Jakobsson E, Fernandez-Rueda J, Lang V, et al. Human mesenchymal stromal cells modulate T-cell responses through TNF-alpha-mediated activation of NF-kappa psi B. *Eur J Immunol*. 2014; 44(2):480–8. doi: [10.1002/eji.201343668](#) PMID: [24307058](#)
13. Nguyen TM, Arthur A, Hayball JD, Gronthos S. EphB and Ephrin-B Interactions Mediate Human Mesenchymal Stem Cell Suppression of Activated T-Cells. *Stem Cells Dev*. 2013; 22(20):2751–64. doi: [10.1089/scd.2012.0676](#) PMID: [23711177](#)

14. Jarvinen L, Badri L, Wettlaufer S, Ohtsuka T, Standiford TJ, Toews GB, et al. Lung resident mesenchymal stem cells isolated from human lung allografts inhibit T cell proliferation via a soluble mediator. *J Immunol*. 2008; 181(6):4389–96. PMID: [18768898](#)
15. Meisel R, Zibert A, Laryea M, Gobel U, Daubener W, Dilloo D. Human bone marrow stromal cells inhibit allogeneic T-cell responses by indoleamine 2,3-dioxygenase-mediated tryptophan degradation. *Blood*. 2004; 103(12):4619–21. PMID: [15001472](#)
16. Corcione A, Benvenuto F, Ferretti E, Giunti D, Cappiello V, Cazzanti F, et al. Human mesenchymal stem cells modulate B-cell functions. *Blood*. 2006; 107(1):367–72. PMID: [16141348](#)
17. Zhang W, Ge W, Li C, You S, Liao L, Han Q, et al. Effects of mesenchymal stem cells on differentiation, maturation, and function of human monocyte-derived dendritic cells. *Stem Cells Dev*. 2004; 13(3):263–71. PMID: [15186722](#)
18. Selmani Z, Naji A, Zidi I, Favier B, Gaiffe E, Obert L, et al. Human leukocyte antigen-G5 secretion by human mesenchymal stem cells is required to suppress T lymphocyte and natural killer function and to induce CD4(+)CD25(high)FOXP3(+) regulatory T cells. *Stem Cells*. 2008; 26(1):212–22. PMID: [17932417](#)
19. Mueller SM, Glowacki J. Age-related decline in the osteogenic potential of human bone marrow cells cultured in three-dimensional collagen sponges. *J Cell Biochem*. 2001; 82(4):583–90. PMID: [11500936](#)
20. Stenderup K, Justesen J, Clausen C, Kassem M. Aging is associated with decreased maximal life span and accelerated senescence of bone marrow stromal cells. *Bone*. 2003; 33(6):919–26. PMID: [14678851](#)
21. Dominici M, Le Blanc K, Mueller I, Slaper-Cortenbach I, Marini FC, Krause DS, et al. Minimal criteria for defining multipotent mesenchymal stromal cells. The International Society for Cellular Therapy position statement. *Cytotherapy*. 2006; 8(4):315–7. PMID: [16923606](#)
22. Jurga M, Forraz N, Basford C, Atzeni G, Trevelyan AJ, Habibollah S, et al. Neurogenic properties and a clinical relevance of multipotent stem cells derived from cord blood samples stored in the biobanks. *Stem Cells Dev*. 2012; 21(6):923–36. doi: [10.1089/scd.2011.0224](#) PMID: [21732816](#)
23. Ali H, Jurga M, Kurgonaitė K, Forraz N, McGuckin C. Defined serum-free culturing conditions for neural tissue engineering of human cord blood stem cells. *Acta Neurobiol Exp (Wars)*. 2009; 69(1):12–23. PMID: [19325637](#)
24. Ali H, Bayatti N, Lindsay S, Dashti AA, Al-Mulla F. Directed differentiation of umbilical cord blood stem cells into cortical GABAergic neurons. *Acta Neurobiol Exp (Wars)*. 2013; 73(2):250–9. PMID: [23823986](#)
25. Kim DW, Staples M, Shinozuka K, Pantcheva P, Kang SD, Borlongan CV. Wharton's Jelly-Derived Mesenchymal Stem Cells: Phenotypic Characterization and Optimizing Their Therapeutic Potential for Clinical Applications. *Int J Mol Sci*. 2013; 14(6):11692–712. doi: [10.3390/ijms140611692](#) PMID: [23727936](#)
26. Fong CY, Chak LL, Biswas A, Tan JH, Gauthaman K, Chan WK, et al. Human Wharton's Jelly Stem Cells Have Unique Transcriptome Profiles Compared to Human Embryonic Stem Cells and Other Mesenchymal Stem Cells. *Stem Cell Rev Rep*. 2011; 7(1):1–16.
27. Hsieh JY, Fu YS, Chang SJ, Tsuang YH, Wang HW. Functional Module Analysis Reveals Differential Osteogenic and Stemness Potentials in Human Mesenchymal Stem Cells from Bone Marrow and Wharton's Jelly of Umbilical Cord. *Stem Cells Dev*. 2010; 19(12):1895–910. doi: [10.1089/scd.2009.0485](#) PMID: [20367285](#)
28. Higuchi O, Okabe M, Yoshida T, Fathy M, Saito S, Miyawaki T, et al. Stemness of human Wharton's jelly mesenchymal cells is maintained by floating cultivation. *Cell Reprogram*. 2012; 14(5):448–55. doi: [10.1089/cell.2012.0020](#) PMID: [22908943](#)
29. Carlin R, Davis D, Weiss M, Schultz B, Troyer D. Expression of early transcription factors Oct-4, Sox-2 and Nanog by porcine umbilical cord (PUC) matrix cells. *Reprod Biol Endocrinol*. 2006; 4:8. PMID: [16460563](#)
30. Nekanti U, Rao VB, Bahirvani AG, Jan M, Totey S, Ta M. Long-term expansion and pluripotent marker array analysis of Wharton's jelly-derived mesenchymal stem cells. *Stem Cells Dev*. 2010; 19(1):117–30. doi: [10.1089/scd.2009.0177](#) PMID: [19619003](#)
31. Ip JE, Wu YJ, Huang J, Zhang LN, Pratt RE, Dzau VJ. Mesenchymal stem cells use integrin beta 1 not CXC chemokine receptor 4 for myocardial migration and engraftment. *Mol Biol Cell*. 2007; 18(8):2873–82. PMID: [17507648](#)
32. Zhu H, Mitsuhashi N, Klein A, Barsky LW, Weinberg K, Barr ML, et al. The role of the hyaluronan receptor CD44 in mesenchymal stem cell migration in the extracellular matrix. *Stem Cells*. 2006; 24(4):928–35. PMID: [16306150](#)

33. Hunsucker SA, Mitchell BS, Spychala J. The 5'-nucleotidases as regulators of nucleotide and drug metabolism. *Pharmacol Therapeut*. 2005; 107(1):1–30.
34. Barker TH, Hagood JS. Getting a grip on Thy-1 signaling. *Bba-Mol Cell Res*. 2009; 1793(5):921–3. doi: [10.1016/j.bbamcr.2008.10.004](https://doi.org/10.1016/j.bbamcr.2008.10.004) PMID: [19007822](https://pubmed.ncbi.nlm.nih.gov/19007822/)
35. Niehage C, Steenblock C, Pursche T, Bornhauser M, Corbeil D, Hoflack B. The cell surface proteome of human mesenchymal stromal cells. *PLoS One*. 2011; 6(5):e20399. doi: [10.1371/journal.pone.0020399](https://doi.org/10.1371/journal.pone.0020399) PMID: [21637820](https://pubmed.ncbi.nlm.nih.gov/21637820/)
36. Duff SE, Li CG, Garland JM, Kumar S. CD105 is important for angiogenesis: evidence and potential applications. *Faseb J*. 2003; 17(9):984–92. PMID: [12773481](https://pubmed.ncbi.nlm.nih.gov/12773481/)
37. Chamberlain G, Fox J, Ashton B, Middleton J. Concise review: Mesenchymal stem cells: Their phenotype, differentiation capacity, immunological features, and potential for homing. *Stem Cells*. 2007; 25(11):2739–49. PMID: [17656645](https://pubmed.ncbi.nlm.nih.gov/17656645/)
38. Deans RJ, Moseley AB. Mesenchymal stem cells: Biology and potential clinical uses. *Exp Hematol*. 2000; 28(8):875–84. PMID: [10989188](https://pubmed.ncbi.nlm.nih.gov/10989188/)
39. Seshareddy K, Troyer D, Weiss ML. Method to isolate mesenchymal-like cells from Wharton's jelly of umbilical cord. *Method Cell Biol*. 2008; 86:101–19. doi: [10.1016/S0091-679X\(08\)00006-X](https://doi.org/10.1016/S0091-679X(08)00006-X) PMID: [18442646](https://pubmed.ncbi.nlm.nih.gov/18442646/)
40. Patel AN, Vargas V, Revello P, Bull DA. Mesenchymal Stem Cell Population Isolated From the Subepithelial Layer of Umbilical Cord Tissue. *Cell Transplant*. 2013; 22(3):513–9. doi: [10.3727/096368912X655064](https://doi.org/10.3727/096368912X655064) PMID: [23057960](https://pubmed.ncbi.nlm.nih.gov/23057960/)
41. Hu L, Hu JQ, Zhao JJ, Liu JR, Ouyang WX, Yang C, et al. Side-by-Side Comparison of the Biological Characteristics of Human Umbilical Cord and Adipose Tissue-Derived Mesenchymal Stem Cells. *Biomed Res Int*. 2013.
42. Nekanti U, Mohanty L, Venugopal P, Balasubramanian S, Totey S, Ta M. Optimization and scale-up of Wharton's jelly-derived mesenchymal stem cells for clinical applications. *Stem Cell Res*. 2010; 5(3):244–54. doi: [10.1016/j.scr.2010.08.005](https://doi.org/10.1016/j.scr.2010.08.005) PMID: [20880767](https://pubmed.ncbi.nlm.nih.gov/20880767/)
43. Dmitrieva RI, Minullina IR, Bilibina AA, Tarasova OV, Anisimov SV, Zaritsky AY. Bone marrow- and subcutaneous adipose tissue-derived mesenchymal stem cells: differences and similarities. *Cell cycle*. 2012; 11(2):377–83. doi: [10.4161/cc.11.2.18858](https://doi.org/10.4161/cc.11.2.18858) PMID: [22189711](https://pubmed.ncbi.nlm.nih.gov/22189711/)
44. Ali H, Forraz N, McGuckin CP, Jurga M, Lindsay S, Ip BK, et al. In vitro modelling of cortical neurogenesis by sequential induction of human umbilical cord blood stem cells. *Stem Cell Rev*. 2012; 8(1):210–23. doi: [10.1007/s12015-011-9287-x](https://doi.org/10.1007/s12015-011-9287-x) PMID: [21678036](https://pubmed.ncbi.nlm.nih.gov/21678036/)
45. Voronova A, Coyne E, Al Madhoun A, Fair JV, Bosiljcic N, St-Louis C, et al. Hedgehog Signaling Regulates MyoD Expression and Activity. *Journal of Biological Chemistry*. 2013; 288(6):4389–404. doi: [10.1074/jbc.M112.400184](https://doi.org/10.1074/jbc.M112.400184) PMID: [23266826](https://pubmed.ncbi.nlm.nih.gov/23266826/)
46. Al Madhoun AS, Mehta V, Li G, Figeys D, Wiper-Bergeron N, Skerjanc IS. Skeletal myosin light chain kinase regulates skeletal myogenesis by phosphorylation of MEF2C. *Embo J*. 2011; 30(12):2477–89. doi: [10.1038/emboj.2011.153](https://doi.org/10.1038/emboj.2011.153) PMID: [21556048](https://pubmed.ncbi.nlm.nih.gov/21556048/)
47. Khadir A, Tiss A, Abubaker J, Abu-Farha M, Al-Khairi I, Cherian P, et al. MAP kinase phosphatase DUSP1 is overexpressed in human obese and modulated by physical activity. *American journal of physiology Endocrinology and metabolism*. 2014:ajpendo 00577 2013.
48. Al Madhoun AS, Voronova A, Ryan T, Zakariyah A, McIntire C, Gibson L, et al. Testosterone enhances cardiomyogenesis in stem cells and recruits the androgen receptor to the MEF2C and HCN4 genes. *J Mol Cell Cardiol*. 2013; 60:164–71. doi: [10.1016/j.yjmcc.2013.04.003](https://doi.org/10.1016/j.yjmcc.2013.04.003) PMID: [23598283](https://pubmed.ncbi.nlm.nih.gov/23598283/)
49. Wang XW, Seed B. A PCR primer bank for quantitative gene expression analysis. *Nucleic Acids Res*. 2003; 31(24).
50. Savage J, Voronova A, Mehta V, Sendi-Mukasa F, Skerjanc IS. Canonical Wnt signaling regulates Foxc1/2 expression in P19 cells. *Differentiation*. 2010; 79(1):31–40. doi: [10.1016/j.diff.2009.08.008](https://doi.org/10.1016/j.diff.2009.08.008) PMID: [19782461](https://pubmed.ncbi.nlm.nih.gov/19782461/)
51. Abu-Farha M, Tiss A, Abubaker J, Khadir A, Al-Ghimlas F, Al-Khairi I, et al. Proteomics analysis of human obesity reveals the epigenetic factor HDAC4 as a potential target for obesity. *PLoS One*. 2013; 8(9):e75342. doi: [10.1371/journal.pone.0075342](https://doi.org/10.1371/journal.pone.0075342) PMID: [24086512](https://pubmed.ncbi.nlm.nih.gov/24086512/)
52. Wang HS, Hung SC, Peng ST, Huang CC, Wei HM, Guo YJ, et al. Mesenchymal stem cells in the Wharton's jelly of the human umbilical cord. *Stem Cells*. 2004; 22(7):1330–7. PMID: [15579650](https://pubmed.ncbi.nlm.nih.gov/15579650/)
53. Karahuseynoglu S, Cinar O, Kilic E, Kara F, Akay GG, Demiralp DO, et al. Biology of stem cells in human umbilical cord stroma: in situ and in vitro surveys. *Stem Cells*. 2007; 25(2):319–31. PMID: [17053211](https://pubmed.ncbi.nlm.nih.gov/17053211/)

54. Nagamura-Inoue T, He H. Umbilical cord-derived mesenchymal stem cells: Their advantages and potential clinical utility. *World J Stem Cells*. 2014; 6(2):195–202. doi: [10.4252/wjsc.v6.i2.195](https://doi.org/10.4252/wjsc.v6.i2.195) PMID: [24772246](https://pubmed.ncbi.nlm.nih.gov/24772246/)
55. Lindenmair A, Hatlapatka T, Kollwig G, Hennerbichler S, Gabriel C, Wolbank S, et al. Mesenchymal stem or stromal cells from amnion and umbilical cord tissue and their potential for clinical applications. *Cells*. 2012; 1(4):1061–88. doi: [10.3390/cells1041061](https://doi.org/10.3390/cells1041061) PMID: [24710543](https://pubmed.ncbi.nlm.nih.gov/24710543/)
56. Wang H, Qiu X, Ni P, Lin X, Wu W, Xie L, et al. Immunological characteristics of human umbilical cord mesenchymal stem cells and the therapeutic effects of their transplantation on hyperglycemia in diabetic rats. *Int J Mol Med*. 2014; 33(2):263–70. doi: [10.3892/ijmm.2013.1572](https://doi.org/10.3892/ijmm.2013.1572) PMID: [24297321](https://pubmed.ncbi.nlm.nih.gov/24297321/)
57. Mennan C, Wright K, Bhattacharjee A, Balain B, Richardson J, Roberts S. Isolation and characterisation of mesenchymal stem cells from different regions of the human umbilical cord. *Biomed Res Int*. 2013; 2013:916136. doi: [10.1155/2013/916136](https://doi.org/10.1155/2013/916136) PMID: [23984420](https://pubmed.ncbi.nlm.nih.gov/23984420/)
58. Mohammadian M, Shamsasenjan K, Lotfi Nezhad P, Talebi M, Jahedi M, Nickkhal H, et al. Mesenchymal stem cells: new aspect in cell-based regenerative therapy. *Adv Pharm Bull*. 2013; 3(2):433–7. doi: [10.5681/apb.2013.070](https://doi.org/10.5681/apb.2013.070) PMID: [24312873](https://pubmed.ncbi.nlm.nih.gov/24312873/)
59. Xu Y, Huang S, Ma K, Fu X, Han W, Sheng Z. Promising new potential for mesenchymal stem cells derived from human umbilical cord Wharton's jelly: sweat gland cell-like differentiative capacity. *J Tissue Eng Regen Med*. 2012; 6(8):645–54. doi: [10.1002/term.468](https://doi.org/10.1002/term.468) PMID: [21916019](https://pubmed.ncbi.nlm.nih.gov/21916019/)
60. Sarugaser R, Hanoun L, Keating A, Stanford WL, Davies JE. Human mesenchymal stem cells self-renew and differentiate according to a deterministic hierarchy. *PLoS One*. 2009; 4(8):e6498. doi: [10.1371/journal.pone.0006498](https://doi.org/10.1371/journal.pone.0006498) PMID: [19652709](https://pubmed.ncbi.nlm.nih.gov/19652709/)
61. Sarugaser R, Ennis J, Stanford WL, Davies JE. Isolation, propagation, and characterization of human umbilical cord perivascular cells (HUCPVCs). *Methods in molecular biology*. 2009; 482:269–79. doi: [10.1007/978-1-59745-060-7_17](https://doi.org/10.1007/978-1-59745-060-7_17) PMID: [19089362](https://pubmed.ncbi.nlm.nih.gov/19089362/)
62. Feldmann RE Jr., Bieback K, Maurer MH, Kalenka A, Burgers HF, Gross B, et al. Stem cell proteomes: a profile of human mesenchymal stem cells derived from umbilical cord blood. *Electrophoresis*. 2005; 26(14):2749–58. PMID: [15971194](https://pubmed.ncbi.nlm.nih.gov/15971194/)
63. Kim J, Shin JM, Jeon YJ, Chung HM, Chae JI. Proteomic validation of multifunctional molecules in mesenchymal stem cells derived from human bone marrow, umbilical cord blood and peripheral blood. *PLoS One*. 2012; 7(5):e32350. doi: [10.1371/journal.pone.0032350](https://doi.org/10.1371/journal.pone.0032350) PMID: [22615730](https://pubmed.ncbi.nlm.nih.gov/22615730/)
64. Munoz J, Low TY, Kok YJ, Chin A, Frese CK, Ding V, et al. The quantitative proteomes of human-induced pluripotent stem cells and embryonic stem cells. *Molecular systems biology*. 2011; 7:550. doi: [10.1038/msb.2011.84](https://doi.org/10.1038/msb.2011.84) PMID: [22108792](https://pubmed.ncbi.nlm.nih.gov/22108792/)
65. Kowno M, Watanabe-Susaki K, Ishimine H, Komazaki S, Enomoto K, Seki Y, et al. Prohibitin 2 regulates the proliferation and lineage-specific differentiation of mouse embryonic stem cells in mitochondria. *PLoS One*. 2014; 9(4):e81552. doi: [10.1371/journal.pone.0081552](https://doi.org/10.1371/journal.pone.0081552) PMID: [24709813](https://pubmed.ncbi.nlm.nih.gov/24709813/)
66. Kurpinski K, Chu J, Wang D, Li S. Proteomic Profiling of Mesenchymal Stem Cell Responses to Mechanical Strain and TGF-beta1. *Cellular and molecular bioengineering*. 2009; 2(4):606–14. PMID: [20037637](https://pubmed.ncbi.nlm.nih.gov/20037637/)
67. Brunner M, Millon-Fremillon A, Chevalier G, Nakchbandi IA, Mosher D, Block MR, et al. Osteoblast mineralization requires beta1 integrin/ICAP-1-dependent fibronectin deposition. *J Cell Biol*. 2011; 194(2):307–22. doi: [10.1083/jcb.201007108](https://doi.org/10.1083/jcb.201007108) PMID: [21768292](https://pubmed.ncbi.nlm.nih.gov/21768292/)
68. Ode A, Kopf J, Kurtz A, Schmidt-Bleek K, Schrade P, Kolar P, et al. CD73 and CD29 concurrently mediate the mechanically induced decrease of migratory capacity of mesenchymal stromal cells. *Eur Cell Mater*. 2011; 22:26–42. PMID: [21732280](https://pubmed.ncbi.nlm.nih.gov/21732280/)
69. Lee HJ, Choi BH, Min BH, Park SR. Changes in surface markers of human mesenchymal stem cells during the chondrogenic differentiation and dedifferentiation processes in vitro. *Arthritis Rheum*. 2009; 60(8):2325–32. doi: [10.1002/art.24786](https://doi.org/10.1002/art.24786) PMID: [19644865](https://pubmed.ncbi.nlm.nih.gov/19644865/)
70. Han HS, Lee S, Kim JH, Seong SC, Lee MC. Changes in Chondrogenic Phenotype and Gene Expression Profiles Associated with the In Vitro Expansion of Human Synovium-Derived Cells. *Journal of Orthopaedic Research*. 2010; 28(10):1283–91. doi: [10.1002/jor.21129](https://doi.org/10.1002/jor.21129) PMID: [20225285](https://pubmed.ncbi.nlm.nih.gov/20225285/)
71. Lehmann GM, Woeller CF, Pollock SJ, O'Loughlin CW, Gupta S, Feldon SE, et al. Novel anti-adipogenic activity produced by human fibroblasts. *Am J Physiol Cell Physiol*. 2010; 299(3):C672–81. doi: [10.1152/ajpcell.00451.2009](https://doi.org/10.1152/ajpcell.00451.2009) PMID: [20554910](https://pubmed.ncbi.nlm.nih.gov/20554910/)
72. Jeong JA, Ko KM, Park HS, Lee J, Jang C, Jeon CJ, et al. Membrane proteomic analysis of human mesenchymal stromal cells during adipogenesis. *Proteomics*. 2007; 7(22):4181–91. PMID: [17994623](https://pubmed.ncbi.nlm.nih.gov/17994623/)